RSC Advances

ROYAL SOCIETY OF CHEMISTRY

www.rsc.org/advances

Use of Porous Cellulose Microcapsules for Water Treatment

Daisy Setyono, Suresh Valiyaveettil*
Department of Chemistry, National University of Singapore, Singapore 117543
E-mail: chmsv@nus.edu.sg

Abstract

Enhanced usage of metal nanoparticles (NPs) in chemical industry and consumer products is causing undesirable environmental pollution, toxicity, and damages to the ecosystem. New methods are needed to remove such emerging pollutants from the environment. In this paper, we report the synthesis and characterization of polyethylenimine coated porous ethyl cellulose microcapsules and show potential application in the extraction of dissolved citrate or PVP-capped Ag NPs and Au NPs from water. The high surface area of the capsules and affinity of amine functional groups towards metal nanoparticles are used to enhance the extraction efficiency. Kinetics, isotherm models, and pH studies were used to understand the observed extraction efficiency of capsules. The capsules showed interesting Langmuir adsorption capacities of 270 mg/g for Ag-citrate, 208 mg/g for Ag-PVP, 116 mg/g for Au-citrate, and 50 mg/g for Au-PVP nanoparticles. We have also developed a simple method to detect metal nanoparticles via modification of the microcapsule with fluorescein isothiocyanate. Overall, our results demonstrate that the porous PEI-crosslinked microcapsule are useful for the extraction of Ag NPs and Au NPs from contaminated water. It can also be modified for the detection of metallic NPs at a ppb level concentration.

KEYWORDS: Water purification; Microcapsule; Adsorbents; Metal nanoparticles; Extraction, Detection

Introduction

Nanomaterials are used in consumer products and industrial manufacturing, owing to the availability of a wide range of nanoparticles in large volumes.[1-3] Increased usage of nanomaterials and unregulated waste disposal is expected to increase the amount of nanoparticles in environment, which enhance the risk of exposure and toxicity to living systems.[4-6] *In vitro* and *in vivo* studies have demonstrated the toxicity of Ag NPs,[9-12] which showed DNA damages and interference with functioning of cell organelles such as mitochondria, and caused significant toxicity to living tissues.[13-15]

The design and characterization of novel adsorbents such as functional polymers and biosorbents for detection and removal of nanopollutants from water is critical for providing clean drinking water to the general population. Only a few methods have been developed for nanopollutants removal from water, such as coagulation and flocculation, flotation, or membrane filtration.[16-20] Adsorbents such as biosorbents, synthetic polymers and metal oxides were developed for the removal of silver (Ag NPs) and gold nanoparticles (Au NPs) from water.[21-26] A practical technology for pollutant removal from water should be cost-effective, efficient, and should not release chemicals into water or environment.

Despite having been used for the removal of pollutants, no report exists on extraction and removal of nanomaterials from water using microcapsules.[27-29] Unlike other known adsorbents, soft microcapsules possess high surface energy, high velocity when dispersed in a fluid,[30] and pack efficiently in a column for large volume application. Polyethylenimine (PEI) under acidic condition binds negatively charged particles and anions via electrostatic interaction.[31,32] Polyvinyl pyrrolidone (PVP) was used as a pore forming agent for ethyl cellulose-coated pellets in earlier studies.[33] This paper highlights

the possibility of using porous, stable and surface functionalized microcapsules for the extraction of dissolved metallic nanoparticles from water. PEI coated and crosslinked porous ethyl cellulose microcapsules were prepared and used for the extraction of Ag NPs and Au NPs from water. Fluorescein isothiocyanate (FITC) functionalized microcapsules are used for the detection of Ag NPs and Au NPs in water. Concept image for the extraction of NPs on PEI-crosslinked porous microcapsule is given in Figure 1.

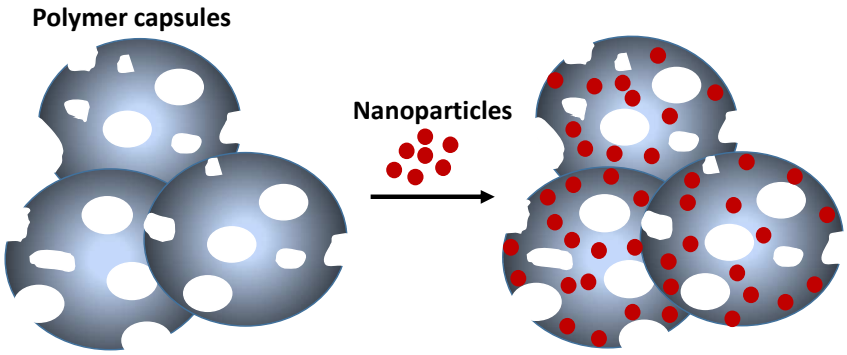

Figure 1. Extraction of Ag NPs or Au NPs using porous polyethylenimine coated ethyl cellulose microcapsules.

Experimental

Materials

Polyvinyl alcohol (PVA) (88% hydrolyzed, M_w = 100 KDa), ethyl cellulose (48% ethoxyl; viscosity = 46 cP, 5% in toluene/ethanol 80 : 20, M_w = 57 KDa), polyvinylpyrrolidone (PVP) (M_w = 10 KDa), sodium dodecyl sulfate (SDS), branched polyethylenimine (PEI) (50% w/v in water, M_n = 60 KDa), glutaraldehyde (50%), phosphoric acid (85%), fluorescein isothiocyanate (FITC), silver nitrate, potassium gold (III) chloride, sodium borohydride, polyvinylpyrrolidone (PVP40) (M_w = 40 KDa), and sodium citrate tribasic dihydrate were purchased from Sigma Aldrich. Chloroform ($CHCl_3$, analytical grade) was purchased from Merck.

Synthesis of Ag and Au NPs

Citrate- and PVP-capped Ag NPs and Au NPs in aqueous solution were prepared using a reported procedure via the reduction of corresponding salts with a reducing agent.[34,35] Sodium citrate tribasic dihydrate (50 mg, 0.017 mmol) dissolved in water (10 mL) was mixed with $AgNO_3$ solution (20 mg in 50 mL water) and stirred at room temperature. Aqueous solution of $NaBH_4$ (10 mg in 9 mL water) was freshly prepared and added dropwise to the silver salt solution. The solution was diluted with water (130 mL) and stirred for a day to make the citrate capped silver nanoparticle (Ag-Cit) solution (2.5×10^{-4} M). The PVP capped silver nanoparticles (Ag-PVPs) were synthesized using a similar procedure with PVP (10 mg) as the capping agent.

Citrate capped gold NPs (Au-Cit) in aqueous solution were prepared using similar procedure as Ag-Cit NPs, using $KAuCl_4.3H_2O$ solution (22 mg in 0.5 mL water) as starting material. Unless otherwise specified, concentration of nanoparticle solution used for extraction studies was kept at 2.5×10^{-4} M.

Preparation of PEI-crosslinked Microcapsules

General procedure for the preparation of microcapsule using water/oil/water double microemulsion method was described elsewhere.[36] According to the procedure reported by Yu et. al., SDS (with polar head group and nonpolar tail) dissolved in chloroform phase forms small water droplets inside the organic phase, which coalesce upon removal of chloroform at the end.

A solution of ethyl cellulose (0.224 g), PVP (0.056 g) and SDS (0.28 g) in chloroform (35 mL) was prepared, added dropwise to an aqueous solution of PVA (1.5 g in 300 mL) and

stirred for 24 hrs at room temperature for complete removal of chloroform. The microcapsules were centrifuged, washed with deionized water (200 mL), and labeled as EC-MC, re-dispersed in 30 ml water containing PEI (0.25 mL), and stirred for 1 h. Crosslinking agent glutaraldehyde (0.6 mL) and phosphoric acid (0.3 mL) were then added drop wise to the solution, stirred for 2 h, microcapsules were collected by centrifugation, washed with deionized water (200 mL), and dried under vacuum at RT for 24 h. The PEI incorporated microcapsules were labeled as PEI-MC.

Modification of PEI-crosslinked Microcapsules with FITC

Dried PEI-MC (0.1 g) was dispersed in water (150 mL) containing FITC (0.03 g) and stirred at room temperature for 24 h. The resulting orange-colored microcapsules were separated by centrifugation, washed with deionized water (200 mL), dried under vacuum at room temperature for 24 h, and labeled as FITC-MC.

Characterization of NPs

Morphology of the NPs synthesized was characterized using Transmission Electron Microscopy (TEM, JEOL JEM 2010, operating at 200 kV). The optical properties were established using UV-Vis spectroscopy (Shimadzu UV-601 PC spectrophotometer). Dynamic light scattering (DLS) and zeta potential measurements were done using a Malvern Zetasizer Nano-ZS instrument.

Characterization of Microcapsules

Fourier transform infrared (FTIR) spectra of the microcapsule before and after functionalization were recorded in the range of 4000 - 400 cm^{-1} using a Bruker ALPHA FT-IR Spectrophotometer, using KBr as matrix. Elemental (CHNS) analysis of the

microcapsule was done before and after functionalization using Elementar Vario Micro Cube instrument. The morphologies of the microcapsules were examined using JEOL JSM-6701F field emission scanning electron microscope (FESEM). Energy dispersive X-ray spectroscopy (EDS) was used for identification of elements on the surface of microcapsule.

Time-dependent Extraction of NPs

To determine the extraction efficiency, microcapsules (0.01 g) were dispersed in Ag NPs or Au NPs solution (10 mL, 10 ppm) and put on an orbital shaker at 250 rpm. Time point collections (0.5 mL) were done every 15, 30, 60, 120, 240, 480 minutes intervals and after 24 h. The solid was removed via centrifugation using ScanSpeed microcentrifuge at 10000 rpm, and the concentration of nanoparticles in solution was quantified using UV-Vis spectroscopy.

Influence of Concentration on Extraction Efficiency

Appropriate amounts of Ag NPs or Au NPs stock solution (2.5×10^{-4} M) was diluted to obtain sample solution in the concentration range of 5 - 100 ppm. Microcapsules (1.2 ± 0.1 mg) were dispersed in the nanoparticle solutions (10 mL) and kept on a shaker for 24 hours. Samples (0.5 mL) were collected, solid was removed by centrifugation, and concentration of nanoparticles in solution was established by UV-Vis spectroscopy.

Effect of pH on NPs adsorption

Ag NPs or Au NPs solutions (10 mL) were adjusted to pH values of 3, 4, 5, 7, 9, and 10 using either 0.1 M NaOH or HCl solutions. Microcapsules (1.2 ± 0.1 mg) were dispersed in nanoparticle solution (10 ml) at different pHs and kept on a shaker for 24 hours to study

the effect of pH on extraction efficiencies. Samples (0.5 mL) were collected, solid was removed by centrifugation, and concentration of nanoparticles in solution was established using UV-Vis spectroscopy.

Desorption Studies

PEI-MC (10 mg) were dispersed in nanoparticle solution (10 mL), put on an orbital shaker at 250 rpm for 24 h, centrifuged, washed with water (200 mL), and solid was dried under vacuum at room temperature. The solid was mixed with dilute HCl (10 mL, 2M) to desorb Ag NPs from the microcapsules, while thiourea (10 mL, 2M) was added to desorb Au NPs, stirred for 24 h, 1.5 mL of the solution was diluted to 7 ml, filtered and analyzed. The microcapsules were centrifuged, solid residue was washed with water (200 mL), dried under vacuum at room temperature, and used for repeated extractions of NPs from water. The process was repeated to check deterioration of extraction efficiency and reusability.

Ag and Au Nanoparticle Detection Using FITC-modified Microcapsules

Ag-Cit, Ag-PVP, and Au-Cit NPs solutions (2 mL) with the concentration range of 10 - 500 ppb were prepared. FITC-MC (1.2 ± 0.1 mg) were dispersed in the nanoparticle solution (2 mL), stirred for 2 h, centrifuged, and the supernatant was analyzed for fluorescence measurement using a Cary Eclipse fluorescence spectrophotometer (excitation and emission wavelengths of 492 nm and 518 nm, respectively). To make a calibration curve, fluorescence intensities of FITC released from the capsule after addition of a known amount of NPs were plotted against the concentration of NPs. The concentration of NPs in unknown sample was determined using this calibration curve.

Results and Discussions

Characterization of Nanoparticles

The nanoparticles (Ag-Cit, Ag-PVP, Au-Cit, Au-PVP) were synthesized by reducing the corresponding Ag or Au salt with $NaBH_4$ and citrate or PVP as capping agents under ambient conditions. In general, the synthesized Au NPs showed narrow size distribution as compared to the Ag NPs (Figure 2A-D). The optical properties of the NPs were characterized using UV-Vis spectroscopy (Figure 2E). Ag-Cit and Ag-PVP NPs have maximum absorption at 390 and 401 nm, respectively, while Au-Cit and Au-PVP NPs showed absorption maxima at 516 nm and 502 nm. These values are consistent with the reported values of NPs synthesized using similar procedure.[37,38]

As expected, DLS data indicated that citrate-capped NPs were smaller in hydrodynamic diameter and more negatively charged than PVP-capped NPs (Figure 2F). The surface charges of nanoparticles decrease in the order, Ag-Cit > Au-Cit > Au-PVP > Ag-PVP. Size distribution of the NPs from the DLS measurements is given in the Supporting Information (Figure S1).

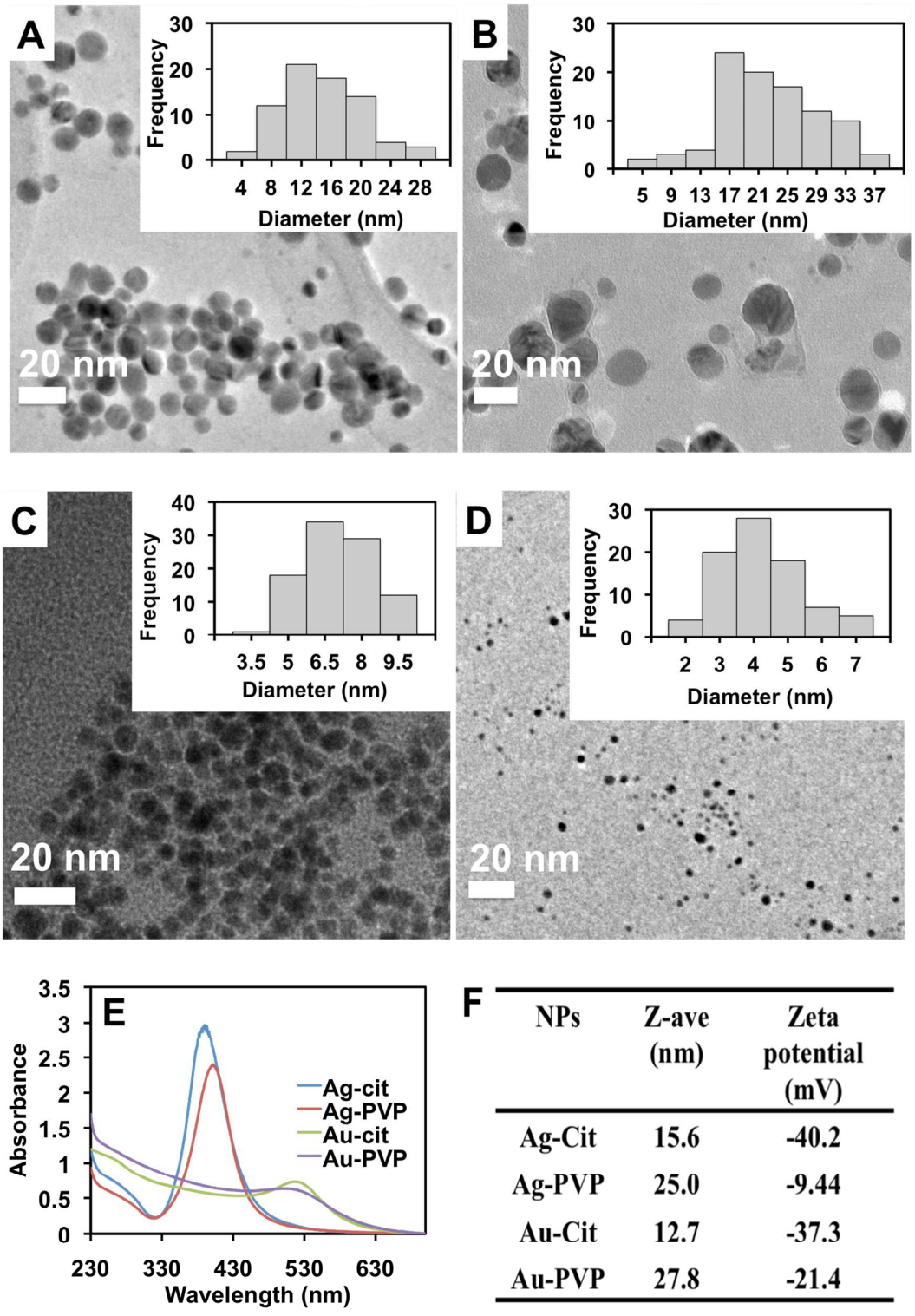

F

NPs	Z-ave (nm)	Zeta potential (mV)
Ag-Cit	15.6	-40.2
Ag-PVP	25.0	-9.44
Au-Cit	12.7	-37.3
Au-PVP	27.8	-21.4

Figure 2. TEM images and size distribution (inset) of Ag-cit (A), Ag-PVP (B), Au-cit (C), Au-PVP NPs (D), UV-Vis absorption spectra of NPs in water (E), hydrodynamic diameter and zeta potential of NPs (F).

Characterization of Microcapsules

The FTIR spectra of microcapsules are given in Figure 3. Peaks centered around 3450 cm^{-1} and 1650 cm^{-1} in the spectra can be attributed to the bending vibration of water molecules bound on ethyl cellulose. In the case of microcapsule functionalized with PEI, a new peak appeared at 1637 cm^{-1} as shown in Figure 3B. After modification with FITC, two new peaks (1598 and 2031 cm^{-1}) that belong to FITC appeared on the spectrum in Figure 3C.[39] The carboxylic acid group on FITC ionizes at pH 7 in water[40-42] and 20% of the amino groups of PEI are protonated at pH 7.[43] Therefore ionic interactions were expected between the COO^- groups of FITC and protonated amino groups of PEI.

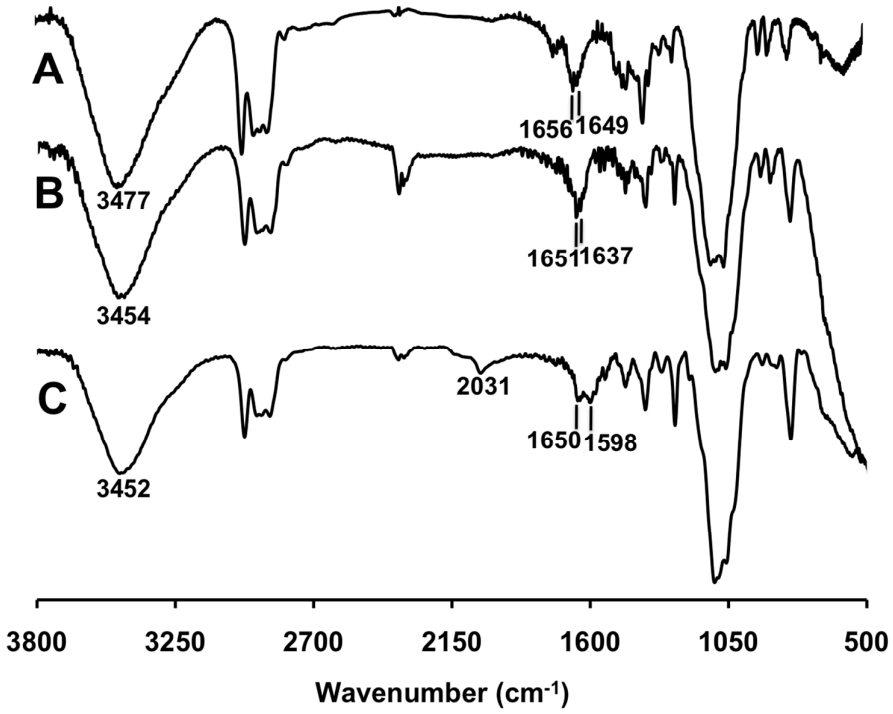

Figure 3. FTIR spectra of EC-MC (A), PEI-MC (B), and FITC-MC (C) using KBr as matrix

Elemental analysis (CHNS) data of the microcapsules are given in Table 1. The nitrogen content was increased from 0.47 to 0.84% upon PEI adsorption, followed by crosslinking

of PEI onto the EC-MC microcapsule. The initial 0.47% of nitrogen from EC-MC originated from PVP adsorbed on the microcapsule. No leaching of PVP or PEI from the capsules was observed upon dispersion into water as the nitrogen content remained the same before and after the extraction. Extraction studies using EC-MC and PEI-MC showed that PEI-MC has much higher extraction capacities towards Ag NPs and Au NPs (Table 1). This indicates that the amine moieties of PEI play a significant role in the extraction of Ag NPs and Au NPs from water.

Table 1. Elemental analysis data and comparison of NPs extraction from water using EC-MC and PEI-MC.

Elemental analysis	**EC-MC**	**PEI-MC**	**FITC-MC**
C	56.18	55.91	54.27
H	8.75	8.38	6.76
N	0.47	0.84	1.21
S	-	-	2.33
Extraction of NPs	**EC-MC**	**PEI-MC**	**FITC-MC**
Ag-Cit (mg/g)	8	272	N/A
Ag-PVP (mg/g)	0	172	N/A
Au-Cit (mg/g)	29	94	N/A
Au-PVP (mg/g)	0	38	N/A

The porosity of the microcapsule provided large surface area for efficient extraction of NPs from water. The size distribution of the microcapsules is from 5 to 30 μm. Morphology of the microcapsule was preserved upon crosslinking of PEI (Figure 4B). NPs adsorbed on the surface of PEI-MC were characterized using SEM (Figure 4C-F) and EDS (Figure S2A-D, Supporting Information). High magnification image of PEI-MC is also given in Supporting Information for comparison (Figure S3). Morphology of NPs was not changed during the extraction and strong electrostatic interaction between positively charged PEI present on the surface and negatively charged citrate-capped NPs is responsible for enhanced extraction efficiency.[44]

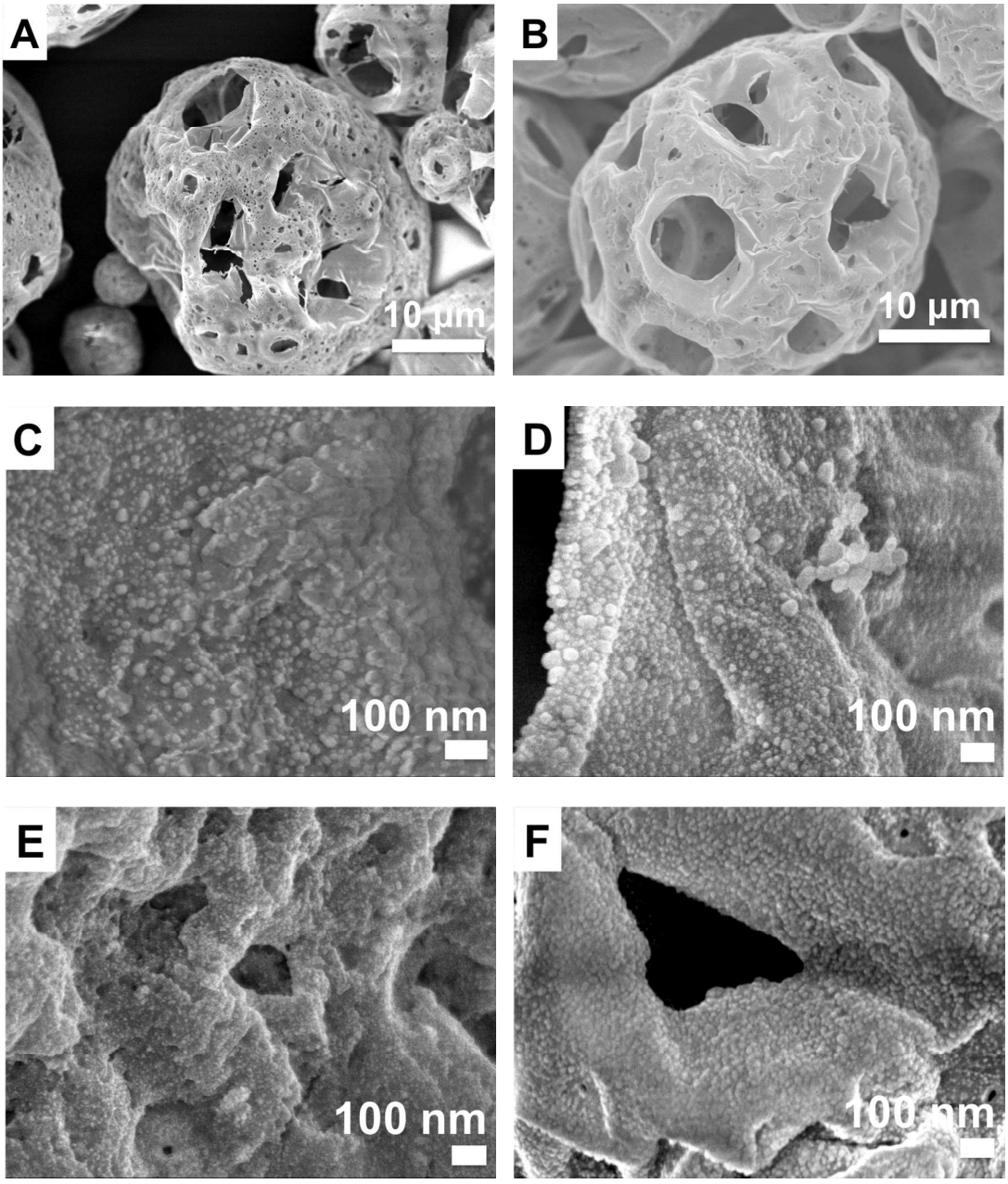

Figure 4. SEM images of EC-MC (A), PEI-MC (B), magnified images of PEI-MC surface after extraction of Ag-Cit (C), Ag-PVP (D), Au-Cit (E), and Au-PVP NPs (F).

Influence of Time on Extraction Efficiency

PEI-MC (1 mg/ml) can be used for the removal of Ag-Cit and Ag-PVP NPs (96%) within 1 - 2 h (Figure 5). However, the removal of Au-Cit and Au-PVP NPs was relatively slower.

Data from the time-dependent studies were used to plot the pseudo-first and pseudo-second order kinetic plots. Extraction of NPs by the capsule reaches a steady state within 4 h.

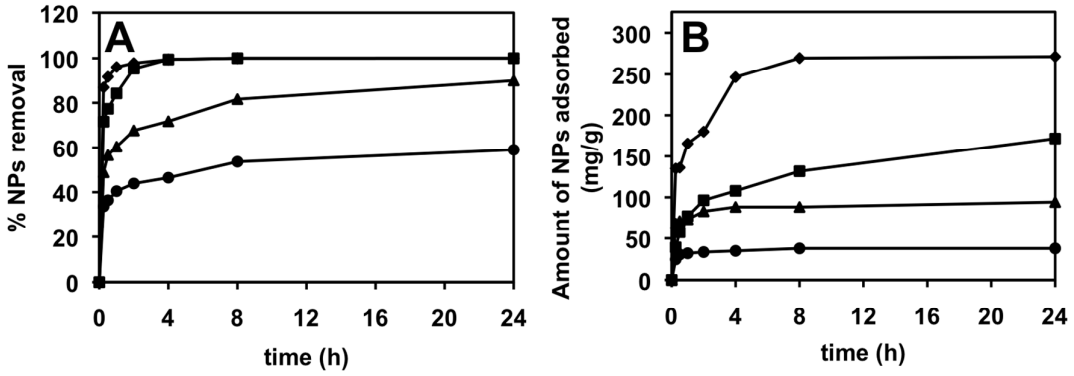

Figure 5. Time-dependent extraction of NPs using 10 mg (A) and 1.0 ± 0.2 mg (B) of PEI-MC in 10 ml nanoparticle solution (◆ Ag-Cit, ■ Ag-PVP, ▲ Au-Cit, ● Au-PVP). Experiments were done at neutral pH and under room temperature.

To characterize the extraction kinetics of NPs, the data (Figure 5) were fitted to both pseudo-first and pseudo-second order kinetic equations. For the pseudo-first order kinetics[45],

$$\log(q_e - q_t) = \log q_e - (k_1/2.303)t \qquad (1)$$

was used, where q_e and q_t describe the amount of NPs adsorbed (mg/g) at equilibrium and at a given time t, while k_1 (min^{-1}) is the pseudo-first order rate constant for the adsorption of NPs.

For the pseudo-second order kinetics[46],

$$t/q_t = t/q_e + 1/(k_2.q_e^2) \qquad (2)$$

was used, where q_e and q_t describe the amount of NPs adsorbed (mg/g) at equilibrium and at a given time, *t*, respectively, while k_2 (g/mg min) is the pseudo-second order rate constant for the adsorption of NPs.

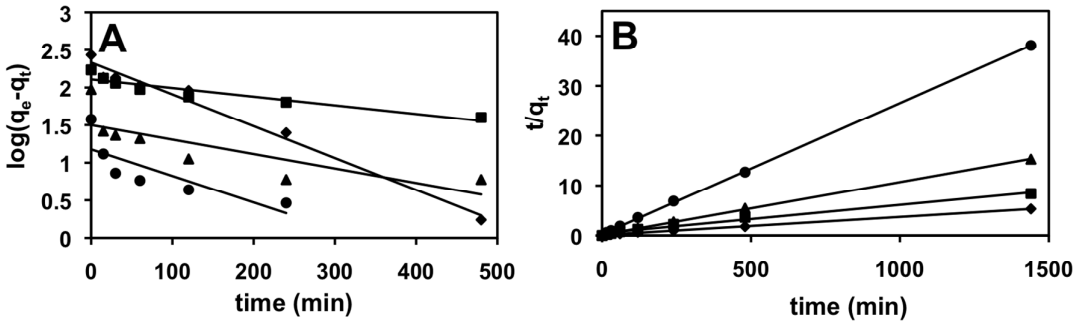

Figure 6. Pseudo-first (A) and pseudo-second (B) order kinetic plots for extraction of NPs using PEI-MC, ◆ Ag-Cit, ■ Ag-PVP, ▲ Au-Cit, ● Au-PVP.

Adsorption of all NPs was better described by pseudo-second order kinetics as indicated by high R^2 values and showed good agreement between calculated and experimental values of q_e (Table 2). This indicates that chemisorption facilitated by electrostatic interaction can be the rate-limiting step for adsorption of Ag NPs and Au NPs on PEI-MC.[47]

Table 2. Pseudo-first and pseudo-second order kinetic parameters for the NPs extraction using PEI-MC.

Nanoparticles		Ag-Cit	Ag-PVP	Au-Cit	Au-PVP
	q_e (exp) (mg/g)	271.49	171.74	94.24	37.79
Pseudo first-order	q_e (mg/g)	214.88	128.59	31.62	15.06
	k_1(min^{-1})	0.010	0.003	0.004	0.008
	R^2	0.9800	0.8790	0.6274	0.6486
Pseudo second-order	q_e (mg/g)	277.78	175.44	94.34	38.02
	k_2(g/mg.min)	0.0001	0.00007	0.0008	0.003
	R^2	0.9984	0.9872	0.9995	0.9998

Concentration-dependent studies

The concentration dependent adsorption data were plotted to fit the widely used Langmuir and Freundlich isotherms. The following equation[48] was used to plot the Langmuir plot:

$$1/Q_e = 1/Q_m + 1/K_L Q_m C_e \qquad (3)$$

where Q_e = amount of adsorbed NPs in mg/g, Q_m = maximum adsorption capacity for monolayer coverage in mg/g, K_L = Langmuir adsorption constant related to heat of adsorption, C_e = initial concentration of NPs in solution.

The measure of how favorable the adsorption process is described by the separation factor (R_L)[49,50] is given by:

$$R_L = 1/(1+ K_L.C_0) \qquad (4)$$

C_0 is the initial NPs concentration (mg/L), $R_L > 1$ indicates unfavorable adsorption; $R_L = 1$ corresponds to a linear adsorption process; $0 < R_L < 1$ indicates favorable adsorption and $R_L = 0$ means irreversible adsorption.

The following equation[51] was used to plot the Freundlich plot:

$$\ln Q_e = 1/n \ln C_e + \ln K_F \qquad (5)$$

where K_F and n are the Freundlich constant and adsorption intensity, respectively.

Adsorption of Ag-Cit, Ag-PVP, Au-Cit, and Au-PVP on microcapsules was better described by Freundlich isotherm and the adsorption of Au-PVP was better suited to Langmuir isotherm model as indicated by the R^2 values (Table 3). This is due to the smaller size and narrow size distribution of Au-PVP NPs. The 1/n values of adsorption of NPs were below 1, which shows chemisorption on heterogeneous binding sites.[52] R_L values for all NPs adsorption were in between 0 to 1, indicating a favorable adsorption process.

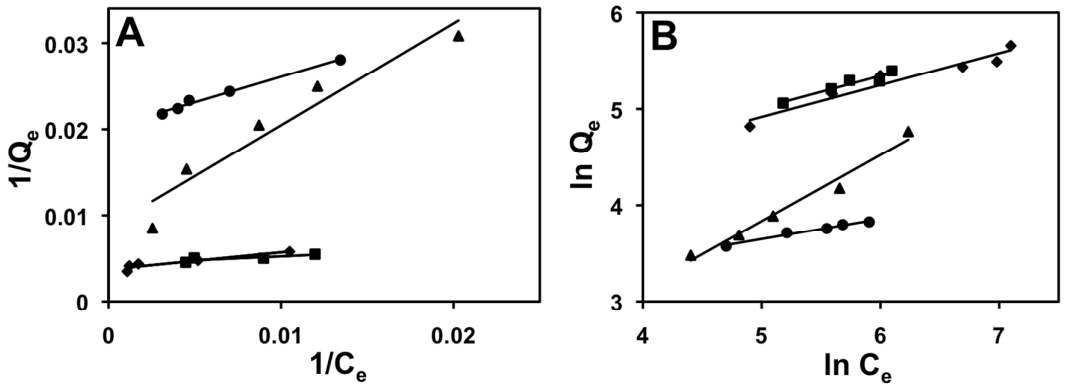

Figure 7. Langmuir (A) and Freundlich (B) isotherm plots. The experiments were done at a microcapsule concentration of 1.0 ± 0.2 mg in 10 ml nanoparticle solution (◆ Ag-Cit, ■ Ag-PVP, ▲ Au-Cit, ● Au-PVP) with a concentration range of 5 - 100 ppm at a constant time of 24 h, at pH of 5 and room temperature.

Table 3. Langmuir and Freundlich parameters from the extraction studies using PEI-MC. Experiments were done at ambient conditions.

Nanoparticles		Ag-Cit	Ag-PVP	Au-Cit	Au-PVP
Langmuir	Q_m (mg/g)	270	208	116	50
	K_L	0.019	0.147	0.007	0.034
	R_L	0.307	0.132	0.729	0.348
	R^2	0.8900	0.8601	0.9279	0.9897
Freundlich	K_F (mg/g)	25.94	28.29	1.49	13.36
	1/n	0.3310	0.3326	0.6867	0.2102
	R^2	0.9389	0.9260	0.9777	0.9803

Q_m values were in the order of: Ag-Cit > Ag-PVP > Au-Cit > Au-PVP (Table 3, row 1). The citrate-capped NPs showed higher extraction capacities than PVP-capped ones owing to their negative surface charges. PEI is a cationic polymer under acidic pH, therefore negatively charged particles are adsorbed onto PEI-MC surface. The extraction of Ag NPs

was more efficient than Au NPs owing to stronger interaction between Ag and amine groups on the surface of microcapsules.[44]

We have also compared the Langmuir adsorption capacities of PEI-MC with other known adsorbents (Table S1, Supporting information).[21-26] PEI-MC showed higher extraction capacities for Ag-Cit, Ag-PVP, and Au-Cit NPs than other adsorbents. Overall, PEI-MC is easier to prepare and environmentally friendly than other adsorbents such as metal oxides reported in literatures[24] and does not contaminate water as it can be readily removed by filtration.

Effect of pH

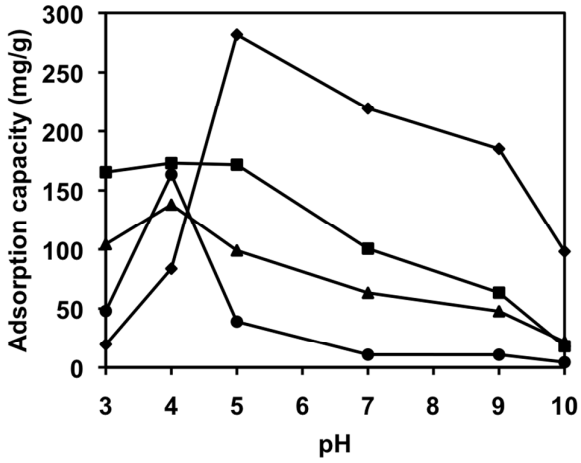

Figure 8. Effect of pH on the extraction of nanoparticles (◆ Ag-Cit, ■ Ag-PVP, ▲ Au-Cit, ● Au-PVP) using PEI-MC. Extractions were done under ambient conditions.

Extraction of Ag NPs and Au NPs was more efficient at acidic pH (Figure 8). This is due to the presence of protonated amine groups on the microcapsule surface at a lower pH. The protonation of PEI increases from 20 to 45% with a decrease in pH from 7 to 5.[53] The optimum pH for the extraction of Ag-Cit NPs (270 mg/g) and Ag-PVP NPs (170 mg/g)

was at pH 5. On the other hand, the optimum extraction of Au-Cit NPs (121 mg/g) and Au-PVP NPs (160 mg/g) was carried out at a pH 4, below which destabilization of NPs occured in solution.

Desorption studies

Desorption experiments were done using nanoparticles adsorbed PEI-MC in 2M HCl (for Ag NPs) or 2M thiourea (for Au NPs) solution, respectively. Percentages of Ag and Au metal content in solution after desorption studies were measured using Dual-view Optima 5300 DV Inductively coupled plasma optical emission spectroscopy (ICP-OES) system. Desorption and extraction processes were done for 3 cycles and the average percentage desorption values are given in Table 4. The mechanism of desorption involves dissolution of Ag and Au NPs adsorbed on PEI-MC to corresponding Ag^+ and Au^+ ions in water under acidic conditions.[54,55] The percentage desorption of Ag-Cit was the lowest among all NPs, indicating strong interaction between Ag-Cit and amine groups on PEI-MC.

Table 4. Desorption studies using 2M HCl for Ag NPs and 2M thiourea for Au NPs from PEI-MC surface.

Nanoparticle	% Desorption
Ag-cit	15
Ag-PVP	50
Au-cit	48
Au-PVP	58

Detection of Ag and Au nanoparticles

A simple detection method was developed for Ag-Cit, Ag-PVP, and Au-Cit using FITC-coated MC. Au-PVP was excluded from this experiment due to lower extraction efficiency.

Fluorescent FITC was immobilized on PEI-MC using electrostatic interaction between the carboxylic group of FITC and protonated amino groups of PEI. Adsorption of FITC on microcapsule increased nitrogen and sulphur content to 1.21 and 2.33, respectively. FITC-MC was only used for detection of NPs and not for extraction because the binding of NPs usually releases FITC into solution.

The principle mechanism of detection involves replacement of FITC on the surface of FITC-MC by Ag NPs or Au NPs as interaction of amino groups with NPs is stronger than that with FITC. No leaching of FITC from the microcapsule was observed in the absence of nanoparticles. UV-Vis measurement also showed no signal of NPs upon release of FITC into solution after extraction.

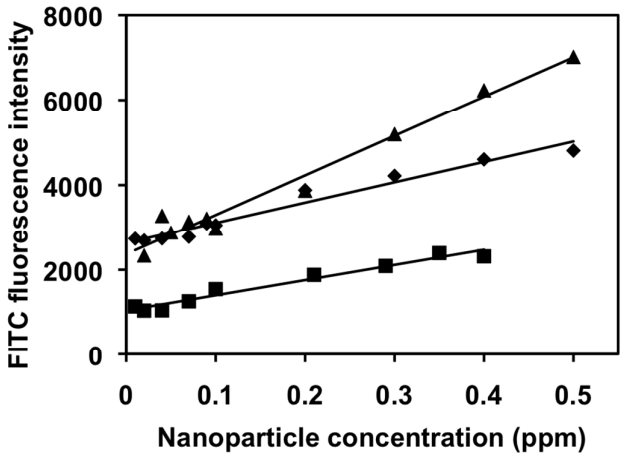

Figure 9. Change in fluorescence intensity of FITC with increasing concentration of Ag/Au nanoparticles against initial Ag or Au nanoparticle concentration in water, ◆ Ag-cit ($y = 4.7669x + 2636.2$, $R^2 = 0.96649$), ■ Ag-PVP ($y = 3.5771x + 1041.1$, $R^2 = 0.96124$), ▲ Au-cit ($y = 9.2762x + 2371.7$, $R^2 = 0.97281$).

Fluorescence intensity of FITC released into water was measured and plotted against initial concentration of Ag NPs or Au NPs (Figure 9). Details on how the equations in Figure 9

were formed can be found in Supporting Information. Even though, the detection time is relatively long at 8 h, this nanoparticle-detection method is simple, much more cost-effective than other single nanoparticle detection methods, has relatively high R^2 values (0.96 - 0.97), and low detection limit. The linear detection range was calculated between 0.01 – 0.5 ppm for Ag-cit and Au-cit and 0.01 – 0.4 ppm for Ag-PVP. Further work is needed to lower the time needed for the detection of NPs, which is necessary for its practical use in water quality monitoring.

Conclusion

In summary, highly porous microcapsules functionalized with PEI are used to extract Ag NPs and Au NPs from water with efficiencies varying from 60 to 99%. Langmuir adsorption capacities of the NPs at pH 5 are given as: 270 mg/g (Ag-Cit), 208 mg/g (Ag-PVP), 116 mg/g (Au-Cit), and 50 mg/g (Au-PVP). The extraction of Ag NPs was more efficient than Au NPs due to differences in their adsorption mechanism. In addition, the extraction of NPs was better at lower pH (i.e. pH 4-5) owing to the presence of protonated amine groups on the microcapsule surface. Upon modification with FITC, the microcapsules were also used for the detection of Ag-cit, Ag-PVP, and Au-cit NPs in solution with the detection limit as low as 0.01 ppm. In addition, we have demonstrated a detection method as a new platform for the detection of metal NPs in water, however more work is needed to shorten the time needed for accurate detection.

Acknowledgements

The authors thank the Ministry of Education for Tier 1 grant and Environment and Water Industry Programme Office (EWI) under the National Research Foundation of Singapore (PUBPP 21100/36/2, NUS WBS no. R-706-002-013-290, R-143-000-458-750, R-143-000-

458-731) for funding support. They also gratefully acknowledge funding and technical support from Department of Chemistry and NUS-Environmental Research Institute, National University of Singapore. DS thanks EWI for a PhD scholarship.

References

1. R. Owen and M. Depledge, Nanotechnology and the environment: risk and rewards, *Mar. Pollut. Bull.*, 2005, **50**, 609-612.
2. M.N. Moore, Do nanoparticles present ecotoxicological risks for the health of the aquatic environment? *Environ. Int.*, 2006, **32**, 967-976.
3. B. Nowack and T.D. Bucheli, Occurrence, behavior and effects of nanoparticles in the environment, *Environ. Pollut.*, 2007, **150**, 5-22.
4. A. Nel, T. Xia, L. Madler and N. Li, Toxic potential of materials at the nanolevel, *Science*, 2006, **311**, 622-627.
5. R. Stelzer and R.J. Hutz, Gold nanoparticles enter rat ovarian granulosa cells and subcellular organelles, and alter in-vitro estrogen accumulation, *J. Reprod. Dev.*, 2009, **55**, 685-690.
6. E. Chang, N. Thekkek, W.W. Yu, V.L. Colvin and R. Drezek, Evaluation of quantum dot cytotoxicity based on intracellular uptake, *Small*, 2006, **2**, 1412-1417.
7. S.K. Das, M.M.R. Khan, T. Parandhaman, F. Laffir, A.K. Guha, G. Sekaran, and A.B. Mandal, Nano-silica fabricated with silver nanoparticles: antifouling adsorbent for efficient dye removal, effective water disinfection and biofouling control, *Nanoscale*, 2013, **5**, 5549-5560.
8. H. Qian, L.A. Pretzer, J.C. Velazquez, Z. Zhao, and M.S. Wong, Gold nanoparticles for cleaning contaminated water, *J. Chem. Tech. Biotech.*, 2013, **88**, 735-741.

9. N. Khlebtsov and L. Dykman, Biodistribution and toxicity of engineered gold nanoparticles: a review of in vitro and in vivo studies, *Chem. Soc. Rev.*, 2011, **40**, 1647-1671.
10. S. Hackenberg, A. Scherzed, M. Kessler, S. Hummel, A. Technau, K. Froelich, C. Ginzkey, C. Koehler, R. Hagen and N. Kleinsasser, Silver nanoparticles: evaluation of DNA damage, toxicity and functional impairment in human mesenchymal stem cells, *Toxicol. Lett.*, 2011, **201**, 27-33.
11. M. Ahamed, M.S. Alsalhi and M.K.J. Siddiqui, Silver nanoparticle applications and human health, *Clin. Chim. Acta*, 2010, **411**, 1841-1848.
12. J.L. Ferry, P. Craig, C. Hexel, P. Sisco, R. Frey, P.L. Pennington, M.H. Fulton, I.G. Scott, A.W. Decho, S. Kashiwada, C.J. Murphy and T.J. Shaw, Transfer of gold nanoparticles from the water column to the estuarine food web, *Nat. Nanotechnol.*, 2009, **4**, 441-444.
13. Y. Teow, P.V. Asharani, M.P. Hande and S. Valiyaveettil, Health impact and safety of engineered nanomaterials, *Chem. Comm.*, 2011, **47**, 7025-7038.
14. J.S. Teodoro, A.M. Simoes, F.V. Duarte, A.P. Rolo, R.C Murdoch, S.M. Hussain and C.M. Palmeira, Assessment of the toxicity of silver nanoparticles *in vitro*: a mitochondrial perspective, *Toxicol. In Vitro*, 2011, **25**, 664-670.
15. C. Wang and S. Valiyaveettil, Correlation of biocapping agents with cytotoxic effects of silver nanoparticles on human tumor cells, *RSC Adv.*, 2013, **3**, 14329-14338.
16. L. Hou, K. Li, Y. Ding, Y. Li, J. Chen, X. Wu, X. Li, Removal of silver nanoparticles in simulated wastewater treatment processes and its impact on COD and NH4 reduction, *Chemosphere*, 2012, **87**, 248-252.

17. D.F. Lawler, A.M. Mikelonis, I. Kim, B.L.T. Lau and S. Youn, Silver nanoparticle removal from drinking water: flocculation/sedimentation or filtration? *Wa. Sci. Technol.*, 2013, **13**, 1181-1187.

18. H. Sajjadi, A. Modaressi, P. Magri, U. Domanska, M. Sindt, J.L. Mieloszynski, F. Mutelet and M. Rogalski, Aggregation of nanoparticles in aqueous solutions of ionic liquids, *J. Mol. Liq.*, 2013, **186**, 1-6.

19. R.J. Honda, V. Keene, L. Daniels and S.L. Walker, Removal of TiO2 nanoparticles during primary water treatment: Role of coagulant type, dose, and nanoparticle concentration, *Environ. Eng. Sci.*, 2014, **31**, 127-134.

20. F. Fu and Q. Wang, Removal of heavy metal ions from wastewaters: a review, *J. Environ. Manage.*, 2011, **92**, 407-418.

21. N. Mahanta and S. Valiyaveettil, Surface modified electrospun poly(vinyl alcohol) membranes for extracting nanoparticles from water, *Nanoscale*, 2011, **3**, 4625-4631.

22. G. Gicheva and G. Yordanov, Removal of citrate-coated silver nanoparticles from aqueous dispersions by using activated carbon, *Colloid. Surface. A.*, 2013, **431**, 51-59.

23. N. Mahanta, W.Y. Leong and S. Valiyaveettil, Isolation and characterization of cellulose-based nanofibers for nanoparticle extraction from an aqueous environment, *J. Mater. Chem.*, 2012, **22**, 1985-1993.

24. R. Mallampati and S. Valiyaveettil, Biomimetic metal oxides for the extraction of nanoparticles from water, *Nanoscale*, 2013, **5**, 3395-3399.

25. B. Dhandayuthapani, R. Mallampati, D. Sriramulu, R.F. Dsouza and S. Valiyaveettil, PVA/Gluten Hybrid Nanofibers for Removal of Nanoparticles from Water, *ACS Sustain. Chem. Eng.*, 2014, **2**, 1014-1021.

26. Z.S. Qureshi, R. DSouza, R. Mallampati and S. Valiyaveettil, Synthesis of amine-functionalized block copolymers for nanopollutant removal from water, *J. Appl. Polym. Sci.*, 2014, DOI: 10.1002/APP.40943.

27. J. Yin, R. Chen, Y. Ji, C. Zhao, G. Zhao and H. Zhang, Adsorption of phenols by magnetic polysulfone microcapsules containing tributyl phosphate, Chemical Engineering Journal, 2010, 157, 466-474.

28. L. Kong, X. Gan, A. L. B. Ahmad, B. H. Hamed, E. R. Evarts, B. Ooi and J. Lim, Design and synthesis of magnetic nanoparticles augmented microcapsule with catalytic and magnetic bifunctionalities for dye removal, Chemical Engineering Journal, 2012, 197, 350-358.

29. X. Ma, Y. Li, X. Li, L. Yang and X. Wang, Preparation of novel polysulfone capsules containing zirconium phosphate and their properties for Pb^{2+} removal from aqueous solution, Journal of Hazardous Materials, 2011, 188, 296-303.

30. B.W. McCormick, in *Aerodynamics, Aeronautics, and Flight Mechanics*, John Wiley & Sons, Inc.; New York, 1979, p. 24.

31. B. Liu and Y. Huang, Polyethyleneimine modified eggshell membrane as a novel biosorbent for adsorption and detoxification of Cr(VI) from water, *J. Mater. Chem.*, 2011, **21**, 17413-17418.

32. M. Owlad, M.K. Aroua and W.M. Wan Daud, Hexavalent chromium adsorption on impregnated palm shell activated carbon with polyethyleneimine, *Bioresour. Technol.*, 2010, **101**, 5098-5103.

33. M. Yang, S. Xie, Q. Li, Y. Wang, X. Chang, L. Shan, L. Sun, X. Huang and C. Gao, Effects of polyvinylpyrrolidone both as a binder and pore-former on the release of sparingly water-soluble topiramate from ethylcellulose coated pellets, *Int. J. Pharm.*, 2014, **465**, 187-196.

34. D.L. Van Hyning, W.G. Klemperer and C.F. Zukoski, Silver nanoparticle formation: Predictions and verification of the aggregative growth model, *Langmuir*, 2001, **17**, 3128-3135.

35. J. Polte, R. Erler, A.F. Thunemann, S. Sokolov, T.T. Ahner, K. Rademann, F. Emmerling and R. Kraehnert, Nucleation and growth of gold nanoparticles studied *via in situ* small angle X-ray scattering at millisecond time resolution, *ACS Nano*, 2010, **4**, 1076-1082.

36. X. Yu, Z. Zhao, W. Nie, R. Deng, S, Liu, R. Liang, J. Zhu, and X, Ji, Biodegradable polymer microcapsules fabrication through a template-free approach, *Langmuir*, 2011, **27**, 10265-10273.

37. J. Polte, T.T. Ahner, F. Delissen, S. Sokolov, F. Emmerling, A.F. Thunemann and R. Kraehnert, Mechanism of gold nanoparticle formation in the classical citrate synthesis method derived from coupled in situ XANES and SAXS evaluation, *J. Am. Chem. Soc.*, 2010, **132**, 1296-1301.

38. D.L. Van Hyning and C.F. Zukoski, Formation mechanisms and aggregation behavior of borohydride reduced silver particles, *Langmuir*, 1998, **14**, 7034-7046.

39. P.C. Pinheiro, C.T. Sousa, J.P. Araujo, A.J. Guiomar and T. Trindade, Functionalization of nickel nanowires with a fluorophore aiming at new probes for multimodal bioanalysis, *J. Colloid Interf. Sci.*, 2013, **410**, 21-26.

40. N. Klonis and W.H. Sawyer, Spectral properties of the prototropic forms of fluorescein in aqueous solution, *J. Fluoresc.*, 1996, **6**, 147-157.

41. J. Yguerabide, E. Talavera, J.M. Alvarez and B. Quintero, Steady-state fluorescence method for evaluating excited-state proton reactions: Application to fluorescein, *Photochem. Photobiol.*, 1994, **60**, 435-441.

42. M.M. Martin and L. Lindqvist, The pH dependence of fluorescein fluorescence, *J. Lumin.,* 1975, **10**, 381-390.

43. J. Suh, H.J. Paik and B.K. Hwang, Ionization of poly(ethyleneimine) and poly(allylamine) at various pH's, *Bioorg. Chem.*, 1994, **22**, 318-327.

44. S. Sanchez-Cortes, R. Marsal Berenguel, A. Madejon and M. Perez-Mendez, Adsorption of polyethyleneimine on silver nanoparticles and its interaction with a plasmid DNA: A surface-enhanced Raman scattering study, *Biomacromolecules*, 2002, **3**, 655-660.

45. J. Febrianto, A.N. Kosasih, J. Sunarso, Y.H. Ju, N. Indraswati and S. Ismadji, Equilibrium and kinetic studies in adsorption of heavy metals using biosorbent: A summary of recent studies, *J. Hazard. Mater.*, 2009, **162**, 616-645.

46. L. Yoshida, T. Konami, Y. Shimonishi, A. Morise and K. Ueno, Adsorption of arsenic(III) ion on various ion exchange resins loaded with Iron(III) and Zirconium(IV), *Nippon Kagaku Kaishi*, 1981, 379-384.

47. T.M. Suzuki, J.O. Bomani, H. Matsunaga and T. Yokoyama, Preparation of porous resin loaded with crystalline hydrous zirconium oxide and its application to the removal of arsenic, *React. Funct. Polym.*, 2000, **43**, 165-172.

48. H. Seki, A. Suzuki and H. Maruyama, Biosorption of chromium(VI) and arsenic(V) onto methylated yeast biomass, *J. Colloid Interf. Sci.*, 2005, **281**, 261-266.

49. G. Limousin, J.P. Gaudet, L. Charlet, S. Szenknect, V. Barthes and M. Krimissa, Sorption isotherms: a review on physical bases, modeling and measurement, *Appl. Geochem.*, 2007, **22**, 249-275.

50. D.G. Krishna and G. Bhattacharyya, Adsorption of methylene blue on kaolinite, *Appl. Clay Sci.*, 2002, **20**, 295-300.

51. A.I. Zouboulis and I.A. Katsoyiannis, Arsenic removal using iron oxide loaded alginate beads, *Ind. Eng. Chem. Res.*, 2002, **41**, 6149-6155.

52. J.Q. Jiang, C. Cooper and S. Ouki, Comparison of modified montmorillonite adsorbents. Part I: Preparation, characterization and phenol adsorption, *Chemosphere*, 2002, **47**, 711-716.

53. H. Wang, Y. Wang and H. Yan, Binding of sodium dodecyl sulfate with linear and branched polyethyleneimines in aqueous solution at different pH values, *Langmuir*, 2006, **22**, 1526-1533.

54. S. Elzey and V.H. Grassian, Agglomeration, isolation and dissolution of commercially manufactured silver nanoparticles in aqueous environments, *J. Nanopart. Res.*, 2010, **12**, 1945-1958.

55. T. Groenewald, The dissolution of gold in acidic solutions of thiourea, *Hydrometallurgy*, 1976, **1**, 277-290.